

Available online at www.sciencedirect.com

ScienceDirect

journal homepage: www.elsevier.com/locate/AJPS

Original Research Paper

High drug loading hydrophobic cross-linked dextran microspheres as novel drug delivery systems for the treatment of osteoarthritis

Zhimin Li^{a,b,c,1}, Xianjing Feng^{a,b,1}, Shixing Luo^{b,d,1}, Yanfeng Ding^{a,b,c}, Zhi Zhang^{a,b,e}, Yifeng Shang^{a,b}, Doudou Lei^{a,b}, Jinhong Cai^{a,b}, Jinmin Zhao^{a,b,e,f,*}, Li Zheng^{a,b,f,*}, Ming Gao^{a,b,f,*}

^a Guangxi Engineering Center in Biomedical Materials for Tissue and Organ Regeneration, The First Affiliated Hospital of Guangxi Medical University, Nanning 530021, China

^b Collaborative Innovation Centre of Regenerative Medicine and Medical BioResource Development and Application Co-constructed by the Province and Ministry, Guangxi Medical University, Nanning 530021, China

^c Department of Spine and Osteopathic Surgery, The First Affiliated Hospital of Guangxi Medical University, Nanning 530021, China

^d Department of Orthopedics, The Ninth Affiliated Hospital of Guangxi Medical University, Beihai, Guangxi 536000, China

^e Department of Orthopaedics Trauma and Hand Surgery, The First Affiliated Hospital of Guangxi Medical University, Nanning 530021, China

^f Guangxi Key Laboratory of Regenerative Medicine, The First Affiliated Hospital of Guangxi Medical University, Nanning 530021, China

ARTICLE INFO

Article history:

Received 7 July 2022

Revised 3 July 2023

Accepted 6 July 2023

Available online 25 July 2023

Keywords:

Sephadex microsphere

Hydrophobic modification

Drug delivery system

High drug loading ratio

Osteoarthritis

ABSTRACT

Drug delivery via intra-articular (IA) injection has proved to be effective in osteoarthritis (OA) therapy, limited by the drug efficiency and short retention time of the drug delivery systems (DDSs). Herein, a series of modified cross-linked dextran (Sephadex, S0) was fabricated by respectively grafting with linear alkyl chains, branched alkyl chains or aromatic chain, and acted as DDSs after ibuprofen (Ibu) loading for OA therapy. This DDSs expressed sustained drug release, excellent anti-inflammatory and chondroprotective effects both in IL-1 β induced chondrocytes and OA joints. Specifically, the introduction of a longer hydrophobic chain, particularly an aromatic chain, distinctly improved the hydrophobicity of S0, increased Ibu loading efficiency, and further led to significantly improving OA therapeutic effects. Therefore, hydrophobic microspheres with greatly improved drug loading ratio and prolonged degradation rates show great potential to act as DDSs for OA therapy.

© 2023 Published by Elsevier B.V. on behalf of Shenyang Pharmaceutical University.

This is an open access article under the CC BY-NC-ND license

(<http://creativecommons.org/licenses/by-nc-nd/4.0/>)

* Corresponding authors at: The First Affiliated Hospital of Guangxi Medical University, Guangxi Engineering Center in Biomedical Materials for Tissue and Organ Regeneration, Nanning 530021, China.

E-mail addresses: zhaojinmin@126.com (J. Zhao), zhengli224@163.com (L. Zheng), gaoming1983125@hotmail.com (M. Gao).

¹ Contributed equally.

Peer review under responsibility of Shenyang Pharmaceutical University.

<https://doi.org/10.1016/j.ajps.2023.100830>

1818-0876/© 2023 Published by Elsevier B.V. on behalf of Shenyang Pharmaceutical University. This is an open access article under the CC BY-NC-ND license (<http://creativecommons.org/licenses/by-nc-nd/4.0/>)

1. Introduction

Osteoarthritis (OA), a progressive joint disease, is characterized by cartilage degeneration, inflammation, subchondral bone sclerosis and osteophyte formation, and will cause pain, joint stiffness and even long-term disability [1–3]. The most widely-prescribed pharmacological treatment for OA is the oral administration of non-steroidal anti-inflammatory drugs (NSAIDs), but the effect is poor as a deficiency of blood vessels in cartilage [4]. Drug delivery systems (DDSs) via intra-articular (IA) injection have confirmed their efficiency in OA therapy, which is helpful to avoid cytotoxicity, short half-life ($T_{1/2}$) and poor utilization rate of the drug caused by oral administration [5,6]. However, the drugs through IA injection are cleared swiftly by the synovium and lymphatic system in the joint cavity [7,8]. Consequently, repeated administrations are required to alleviate pain and joint inflammation, which may cause adverse effects [9]. To prolong the retention of local drugs, it is necessary to develop IA DDSs.

Among various DDSs, hydrogels, from natural polysaccharides such as hyaluronic acid (HA), chitosan, dextran, etc., are endowed with good biocompatibility, biodegradability, non-toxicity and non-immunogenic, especially their lubrication effect for cartilage, and have been widely used for OA therapy [10–13]. However, the non-uniform shape and large size of hydrogels [14] may cause damage to the surrounding tissue and discomfort for the patient. Additionally, rapid degradation and clearance of natural polysaccharides *in vivo* [15] limited their further application. An alternative is the use of hydrogel microspheres which are injectable [16], allowing them to perfectly fill the space in the joint cavity. In addition, the hydrogel microspheres usually have higher porosity than the conventional microparticles, with the advantages of drug-loading efficiency and release kinetics [17].

Sephadex (S0), a cross-linked and porous dextran hydrogel microsphere, whose hydrolysis is glucose, has renewable sourcing, little immunogenicity/cytotoxicity, and excellent biocompatibility [18–20], which is a potential DDS for IA injection [21,22]. An investigation revealed that the $T_{1/2}$ of dextran was 5–17 h in OA joints, which might impact the long-term therapeutic effect [7]. S0 could improve the retention time in the cavity due to its cross-linked three-dimensional network and slow degradation. It was reported that S0 acted as a carrier to avoid rapid clearance in the nasal cavity, demonstrating its excellent biocompatibility and controlled drug release [23]. In addition, as a commercial product, S0 is relatively uniform in size and crosslinking degree. However, similar to most natural polysaccharides, S0 with abundant hydroxyl groups showed high hydrophilicity, resulting in a low drug-loading ratio [17]. Generally, hydrophobic domains in the DDSs determined drug loading efficiency and the corresponding release of hydrophobic drugs, due to the hydrophobic interaction between drugs and hydrophobic domains [24]. To improve the hydrophobicity of DDSs, it was commonly suggested to graft hydrophobic groups such as alkyl or aromatic chains [25,26]. Hou et al. demonstrated that the porous octyl dextran microspheres with a higher degree

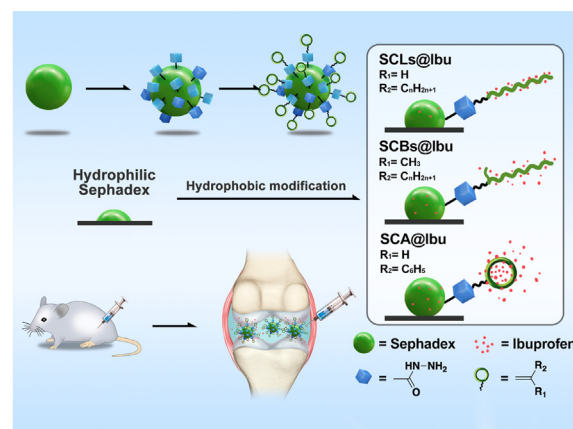


Fig. 1 – Schematic illustration of the fabrication of hydrophobic microspheres with different hydrophobicity and they acted as DDSs after Ibu loading for OA therapy in cartilage cavity.

of substitution (DS) showed higher hydrophobicity and drug loading efficiency than those with lower DS [17]. However, the hydrophobic domains were affected by various types of alkyl chains, and the hydrophobicity increased with the increase of alkyl chain length revealed by the water contact angle (WCA). Specifically, the WCA of modified polyvinyl alcohol (PVA) films increased obviously, with $62.8 \pm 4.9^\circ$ for C3, $76.6 \pm 0.2^\circ$ for C6, and $83.3 \pm 0.6^\circ$ for C9, compared to PVA ($59.4 \pm 6.8^\circ$) [27]. Simultaneously, some investigations also revealed that a branched alkyl chain could decrease surface energy to increase hydrophobicity [28]. Besides, the introduction of aromatic groups in dextran could adsorb more hydrophobic substances due to the π - π stacking interactions [29]. Thus, linking with hydrophobic groups might increase the hydrophobicity of S0 and further improve drug loading. Furthermore, alkyl chain length and aromatic chain should also be considered as factors affecting hydrophobicity.

In this study, we innovatively fabricated a series of modified S0 grafted with alkanes or aromatics by carbazate-mediated Schiff-base reaction as DDSs for OA therapy. We also investigated the impact of linear alkyl chain length, branched alkyl chain length, and aromatic chain on the hydrophobicity and therapeutic effect of modified microspheres. Briefly, S0 was firstly modified by carbazate to obtain carbazate modified S0 (SC), followed by the Schiff-base reaction to form three types of S0 derivatives: (1) SC reacted with aliphatic aldehydes to obtain linear alkanes-modified SC (SCLs) with different length of alkyl chains including SCL1, SCL2, SCL3. (2) SC reacted with alkanones to obtain branched alkanes-modified SC (SCBs) with different lengths of alkyl chains including SCB1, SCB2, SCB3. (3) SC reacted with benzaldehyde to form aromatic modified SC (SCA). Furthermore, the modified microspheres including SCLs, SCBs and SCA were loaded with ibuprofen (Ibu), by hydrophobic interaction to generate three types of DDSs (SCL@Ibu, SCB@Ibu and SCA@Ibu). Finally, the therapeutic effects of these DDSs were investigated based on IL-1 β induced chondrocytes *in vitro* and OA rats *in vivo*. Fig. 1 illustrated the schematic procedures of the fabrication

of hydrophobic microspheres and they acted as DDSs after Ibu loading for OA therapy *in vivo*.

2. Materials and methods

2.1. Materials

S0 was purchased from Amersham Biosciences. Dimethyl sulfoxide (DMSO, $\geq 99.9\%$), tert-butyl carbazate ($\geq 98.0\%$), hydrazine hydrate (80%), 1, 1'-carbonyldiimidazole (CDI, $\geq 97.0\%$), 2, 4, 6-trinitrobenzene sulfonic acid (TNBS, 5% (w/v) in H₂O), phosphate buffer saline (PBS, pH 7.4), sodium dihydrogen phosphate (NaH₂PO₄), sodium hydroxide (NaOH), acetaldehyde (99.5%), butyraldehyde (99%), butanone (99.7%), hexaldehyde (98%), 2-hexanone (98%) and ibuprofen ($\geq 98\%$) were obtained from Sigma Aldrich. Benzaldehyde (99.9%) and acetone (99%) were commercially obtained from Fisher Scientific. All chemicals were used directly without further purification.

2.2. Synthesis of SC

S0 (1 g) was dispersed with DMSO (20 ml) by shaking for 15 min on a shaker. The mixed solution was stirred for 24 h after the addition of CDI (8 g). Subsequently, the mixture was rinsed with deionized water and centrifuged (500 rpm, 5 min) for three times. Finally, the product was collected by lyophilization.

2.3. Preparation of hydrophobic S0

SC (0.3 g) was dispersed in DMSO (10 ml) for 15 min with shaking, followed by adding acetaldehyde (88 μ l), butyraldehyde (144 μ l), hexaldehyde (200 μ l), acetone (116 μ l), butanone (164 μ l), 2-hexanone (200 μ l), and benzaldehyde (212 μ l), respectively. The mixtures reacted for another 24 h and were then washed with DMSO for three times. After washing with methanol, the final products were obtained by lyophilization. And the detailed reaction condition was illustrated in Table S1.

2.4. Basic characterization

The samples were investigated by using Fourier transform infrared spectra (FTIR, PerkinElmer, USA) and X-ray photoelectron spectroscopy (XPS, Physical Electronics, USA). The thermal stability of microspheres was investigated by implementing thermogravimetric analysis (TGA) using TA instruments (TGAQ500). And the samples were heated from room temperature to 800 °C with an increase of 5 °C/min under the N₂ atmosphere. The morphology of microspheres was characterized using a scanning electron microscope (SEM) coupling with an energy dispersive spectrometer (EDS) (Zeiss, Germany) after gold coating. The DS of carbazate groups, defined as the content of carbazate groups per dextran unit, was identified by TNBS assay [30]. Briefly, SC (10 mg) was immersed in 1 ml sodium tetraborate decahydrate buffer (pH 9.3, 0.1 M), and mixed with TNBS solution (25 μ l) for 3 h. Then

the absorbance of the mixture was detected at 340 nm by UV-vis spectroscopy (Shimadzu, Japan). The standard curves were based on various concentrations of tert-butyl carbazate solution. The DS of SC was also calculated by the elemental ratio of XPS.

Besides, the pH stability of microspheres was tested according to the previous method [31]. Briefly, S0 or SC (10 mg) were separately immersed in PBS at pH 1, 2.5, 5.5 or 7.4 for 96 h. The absorbance of buffer solutions was detected at the predetermined time points (1, 2, 6, 24, 48 and 96 h) by TNBS assay.

The hydrophobic properties of microspheres were investigated by a video-based optical contact angle measuring system (OCA15EC, Data physics, Germany). Briefly, microspheres were placed on the platform by double side tape for WCA measurements with a droplet of 2.5 μ l/s.

2.5. Degradation rate *in vitro*

The degradation rate of microspheres was measured by the gravimetric method. Details: microspheres were placed in pre-weighed EP tubes and incubated in different PBS (pH 5.5 and 7.4) with shaking (37 °C, 80 rpm), corresponding to the pH of synovial fluid from OA joint. At predetermined time points (1, 3, 7, 14, 21 and 28 d), samples were freeze-dried and weighed to determine their residual weight.

The resistance of microspheres to enzymatic degradation was evaluated by using a dextranase assay. Briefly, microspheres were incubated in different PBS (pH 5.5 and 7.4) containing dextranase (2 U/ml) with shaking (37 °C, 80 rpm), to simulate the physiological conditions of the cartilage cavity. The supernatant was replaced every 2 d and the medium was replenished with freshly prepared enzyme solution. At the designated time points, samples were freeze-dried and weighed to determine their residual weight. The degradation rate was calculated according to the following equation:

$$\text{Degradation rate(\%)} = (W_0 - W_t) / W_0 \times 100\%$$

Where W_0 referred to the initial dry weight of microspheres, and W_t referred to the freeze-dried weight of microspheres at the given time points.

2.6. Drug loading ratio and release rate

The microspheres (10 mg) were dispersed in PBS (4 ml), followed by adding Ibu solution (1 ml, 10 mg/ml in methanol). The mixtures were placed in the shaker (20 °C, 80 rpm) for 24 h till the total evaporation of methanol. After washing three times with PBS, the final products were re-dispersed in the solution of methanol and PBS (1: 1, v/v, 1 ml), and the solution was studied by UV-vis spectroscopy (Shimadzu, Japan) at 222 nm. The Ibu standard curve was established based on Ibu solutions in various concentrations. The drug entrapment efficiency (EE) and loading efficiency (LE) were calculated using Eqs. (1) and (2), respectively.

$$\text{EE(\%)} = \frac{\text{Mass of drug entrapped in microspheres}}{\text{mass of drug fed}} \times 100\% \quad (1)$$

$$\text{LE(\%)} = \frac{\text{Mass of drug entrapped in microspheres}}{\text{mass of microspheres with drug entrapped}} \times 100\% \quad (2)$$

Meanwhile, the investigation of drug release rate was implemented as following: Ibu-loaded microspheres (10 mg) were dispersed with PBS (1 ml) in a dialysis bag (3.5 K MWCO, Thermo Fisher) and then immersed in a glass bottle containing PBS (pH 7.4, 50 ml) with 1% Tween 80. The release study was performed in the incubator shaker (37 °C, 80 rpm). At selected time points (1, 2, 4, 8, 24, 48, 96 and 192 h), 0.5 ml aliquots were removed and replenished with the same volume of release medium. The absorbance value of samples was recorded by UV-vis spectroscopy at 222 nm. And the concentrations of Ibu were analyzed according to the corresponding Ibu standard curve and the drug release rate was further calculated.

2.7. Isolation and culture of chondrocytes

The primary chondrocytes were extracted from knee joints of five-day-old Sprague-Dawley (SD) rats which were provided by the Animal Experimental Center of Guangxi Medical University. Especially, the specific operation was conducted as described previously [32]. The Dulbecco's modified eagle medium (DMEM, Gibco, USA) containing 1% (v/v) penicillin/streptomycin (Solarbio, China) and 10% (v/v) fetal bovine serum (Gibco, USA) was changed every 3 d. Chondrocytes were passaged when reaching 80%–90% confluence. Subsequently, the third passage cells were utilized for further experiments.

2.8. Cytotoxicity of microspheres

The cell cytotoxicity of Ibu and Ibu-loaded microspheres was detected by using cell counting kit-8 (CCK-8, Dojindo, Japan). Briefly, chondrocytes were seeded in 96-well plates with a density of 8,000 cells per well, and the medium was replaced with fresh culture medium with Ibu (0, 6.25, 12.5, 25, 50, 100, 200, 400 and 800 µg/ml). After incubation for another 48 h, the chondrocytes were rinsed with PBS for three times and replaced with medium containing 10% CCK-8 solution (100 µl). The absorbance was recorded at 450 nm in a microplate spectrophotometer (Thermo Fisher, USA). To obtain the relative cell viability, the absorbance of other groups was compared with the control group. Furthermore, the protective effects of Ibu-loaded microspheres in IL-1 β (10 ng/µl, 24 h) induced chondrocytes were also tested by CCK-8 assay. All experiments were repeated in triplicates.

Besides, Live/dead staining was conducted using a Calcein-AM/PI assay kit (Sigma, USA). The chondrocytes were incubated with calcein and propidium iodide (PI) for 5 min in the darkness. After rinsing with PBS, the live/dead cells were imaged by a microscope (Olympus BX53, Tokyo, Japan).

2.9. Quantitative real-time polymerase chain reaction (qRT-PCR)

The gene expression levels of MMP-3, MMP-13, COX-2 and IL-6 were quantified by qRT-PCR. The total RNA of chondrocytes was isolated by RNA extraction kit (Magen, China) according

to the manufacturer's protocol. The qRT-PCR reactions were conducted using a LightCycler® System (Roche, Switzerland) as previously described [33]. The primer sequences were presented in Table S1. The relative gene expression levels were analyzed by the $2^{-\Delta\Delta CT}$ method and normalized to glyceraldehyde-3-phosphate dehydrogenase (GAPDH).

2.10. Intracellular protein detection

The expression of MMP-3, MMP-13, COX-2 and IL-6 at the protein level was explored by enzyme-linked immunosorbent assay (ELISA, Meimian, China). Briefly, chondrocytes induced with IL-1 β (10 ng/µl, 24 h) were co-cultured with different Ibu-loaded microspheres for 24 h and the total proteins were extracted with RIPA lysis buffer (Solarbio, China). And the targeting proteins were detected by the corresponding ELISA kit following the standard operation procedure. Finally, the absorbance of samples was obtained at 450 nm by a microplate reader (Thermo Fisher, USA).

2.11. Anti-inflammatory and chondroprotective activity in vitro

Chondrocytes were seeded in 6-well plates with a density of 3×10^5 cells per well and pre-treated with IL-1 β (10 ng/µl) for 24 h, followed by the addition of Ibu-loaded microspheres for 24 h. The chondrocytes were fixed with 95% ethanol for 15 min after rinsing with PBS for 3 times. The staining with hematoxylin and eosin (HE, Solarbio, China) or 0.1% Safranin-O (Solarbio, China) was performed to assess the cell morphology and the content of glycosaminoglycans (GAGs), respectively. The images were finally captured by a microscope (Olympus BX53, Tokyo, Japan).

The expression levels of inflammatory cytokines (MMP-13 and IL-6) in chondrocytes were evaluated using immunofluorescent staining. Cell samples were cultured for 24 h and fixed with 95% ethanol for 15 min. And cells were blocked by goat serum for 15 min after incubating with 3% H₂O₂ for 15 min. Subsequently, the above samples were incubated with the primary antibody of MMP-13 or IL-6 (1:200 dilution, Boster, China) at 4 °C overnight. The secondary antibody FITC-anti-rabbit IgG (Boster, China) was added for 1 h in the darkness. Later, nuclei staining was performed with DAPI (1:1,000 dilution, Solarbio, China). The images were finally obtained by a fluorescence microscope (Olympus BX53, Japan).

2.12. Proliferation and biochemical analyses of chondrocytes

Chondrocytes were induced by IL-1 β (10 ng/µl) for 24 h followed by incubation with Ibu-loaded microspheres for another 24 h. The collected chondrocytes were resuspended with PBS (1 ml), added with proteinase K (1 µl, 20 mg/ml, Biosharp, China), and further incubated at 58 °C for 10 h. After the addition of Hoechst 33258 (Solarbio, China), the fluorescent intensity of samples was detected by a microplate reader (BioTek, USA) at 460 nm using calf thymus DNA as the standard. The content of GAGs was investigated by the 1, 9-dimethylmethylene blue (DMMB, Sigma, USA) method.

The samples were mixed with DMMB solution into 96-well plates and the absorbance was recorded at 525 nm using a microplate reader (Thermo Fisher, USA).

2.13. OA therapy in vivo

One hundred and fifty 8-week-old male rats (250 ± 10 g) were chosen to implement the treatment experiments *in vivo*. The animal experiments were approved from the Animal Ethics Committee of Guangxi Medical University and followed the Guide of Care and Use of Laboratory Animals. In order to establish the OA model *in vivo*, the rats were operated by anterior cruciate ligament transection (ACLT) after anesthesia with 2% pentobarbital sodium (40 mg/kg). The sham group was operated on rat knees only with incisions of the skin and joint capsule. And the OA rats were obtained after ACLT for 4 weeks.

In order to investigate the retention time of the drug in the articular cavity, ninety OA SD rats were randomly divided into five groups ($n = 3$): ibuprofen (Ibu), S0@Ibu, SCL3@Ibu, SCB3@Ibu and SCA@Ibu, and received IA administration with the above formulations (728 $\mu\text{g}/\text{ml}$, 100 μl). The synovial fluids were collected at 2 h, 12 h, 24 h, 48 h, 96 h after administration and stored at -80°C . The synovial fluids were thawed at room temperature before analysis. The synovial fluids (50 μl) were added 0.1 mol/l NaOH methanol solution (50 μl) and methanol (100 μl), vortexing for 3 min. The mixed solutions were centrifuged for 10 min at 4,000 r/min, and their supernates were filtered by millipore filter (0.22 μm), and then subjected to high performance liquid chromatograph (HPLC, Shimadzu LC-20AB, Japan) analysis. The samples were separated on C_{18} column (250 mm \times 4.6 mm, 5 μm , Feinigen XPeonyx C18-S, China) and eluted with an elution of 20% solvent A (water containing 0.1% trifluoroacetic acid) and 80% solvent B (methanol) at column temperature 35°C , by the flow rate 1.0 mL/min and detection wavelength 263 nm. The ibuprofen contents in synovial fluids were calculated by the calibration curves.

Sixty OA SD rats were randomly separated into five groups ($n = 6$): saline, S0@Ibu, SCL3@Ibu, SCB3@Ibu, and SCA@Ibu, and received IA administration with the above formulations (728 $\mu\text{g}/\text{ml}$, 100 μl) once a week till 4 weeks. After IA injection, the rats were sacrificed and knee joints were harvested for further study at 2 and 4 weeks. The knee joints were photographed and evaluated based on Pelletier's macroscopic scoring [34]. In order to investigate the levels of inflammatory factors (MMP-13 and IL-6) in the knee joints, the synovial fluid was collected and measured using the commercially available ELISA kit (Meimian, China) following the standard operation procedure. The absorbance of products was obtained at 450 nm by a microplate reader (Thermo Fisher, USA).

Furthermore, the knee joints, heart, liver, spleen, lungs, and kidney of rats were fixed using 4% paraformaldehyde for 48 h. Specifically, the knee joints were decalcified in 10% ethylenediaminetetraacetic acid (EDTA, Solarbio, China) buffer solution using Ultrasonic Decalcifying Unit (USE 33, Medite, Germany) for 4 weeks. Furthermore, the samples were embedded in paraffin and sliced into 5 μm tissue sections. The HE staining and Safranin-O fast green (Solarbio, China) staining were conducted for knee tissue sections.

The sections were observed by using a microscope (Olympus BX53, Japan) and the improved Mankin's score system was applied to evaluate cartilage degeneration as previously described [35].

Finally, immunohistochemical staining was performed to identify the expression of MMP-13 and IL-6 in the knee joint. Briefly, the knee sections were incubated with 3% H_2O_2 for 15 min and blocked by goat serum for another 15 min at room temperature. Subsequently, knee sections were incubated with the primary antibody of MMP-13 or IL-6 (1: 200 dilution, Boster, China) at 37°C for 90 min in the humidified chamber. After rinsing three times with PBS, knee sections were incubated with the biotin-labeled goat anti-mouse/rabbit IgG (ZSGB Bio, China) for 30 min. Later, samples were counterstained with hematoxylin after staining with 3, 3'-diaminobenzidine tetrahydrochloride (DAB, Boster, China). Finally, the tissue sections sealed with neutral resin were imaged using the upright microscope.

2.14. Statistical analysis

The data were analyzed by SPSS 20.0 (SPSS Inc., Chicago, Illinois, USA) and presented as mean \pm standard deviation. All experiments were carried out at least in triplicates. The differences between the two groups were analyzed with one-way ANOVA followed by the Least Significant Difference (LSD) analysis or Game Howell analysis. It was identified as statistically significant when $P < 0.05$.

3. Results and discussion

3.1. Synthesis of hydrophobic microspheres

The hydroxyl groups of S0 were first activated by CDI and then reacted with hydrazine to obtain SC. Furthermore, based on the Schiff-base reaction between carbazate groups and carbonyl compounds, SC reacted with acetaldehyde, butanal, and hexaldehyde respectively to obtain a series of linear alkanes modified S0 with increased carbon chain lengths (SCL1, SCL2, and SCL3). Similarly, SC reacted with acetone, butanone and 2-hexanone, respectively, to obtain branched alkanes modified with increased carbon chain lengths (SCB1, SCB2, and SCB3). Besides, SC reacted with benzaldehyde to form aromatic hydrocarbon-modified SC, named SCA (Fig. 1).

3.2. Basic characterization of hydrophobic microspheres

FTIR results of microspheres were illustrated in Fig. 2A. The peak at 1710 cm^{-1} corresponding to $\text{C}=\text{O}$ of the carbazate group was observed for SC, SCLs, SCBs and SCA, compared to S0. It was clearly found that SC and its derivatives were successfully modified with carbazate groups. Besides, the microspheres were further investigated by XPS. As presented in Fig. 2B, the apparent peak at 397 eV corresponding to N element ($-\text{NHNH}_2$) was observed for SC, SCLs, SCBs and SCA instead of S0. It also provided the proof of successful modification of carbazate groups for microspheres.

The surface morphology of microspheres was investigated using SEM-EDS (Fig. 2C). The diameter of microspheres

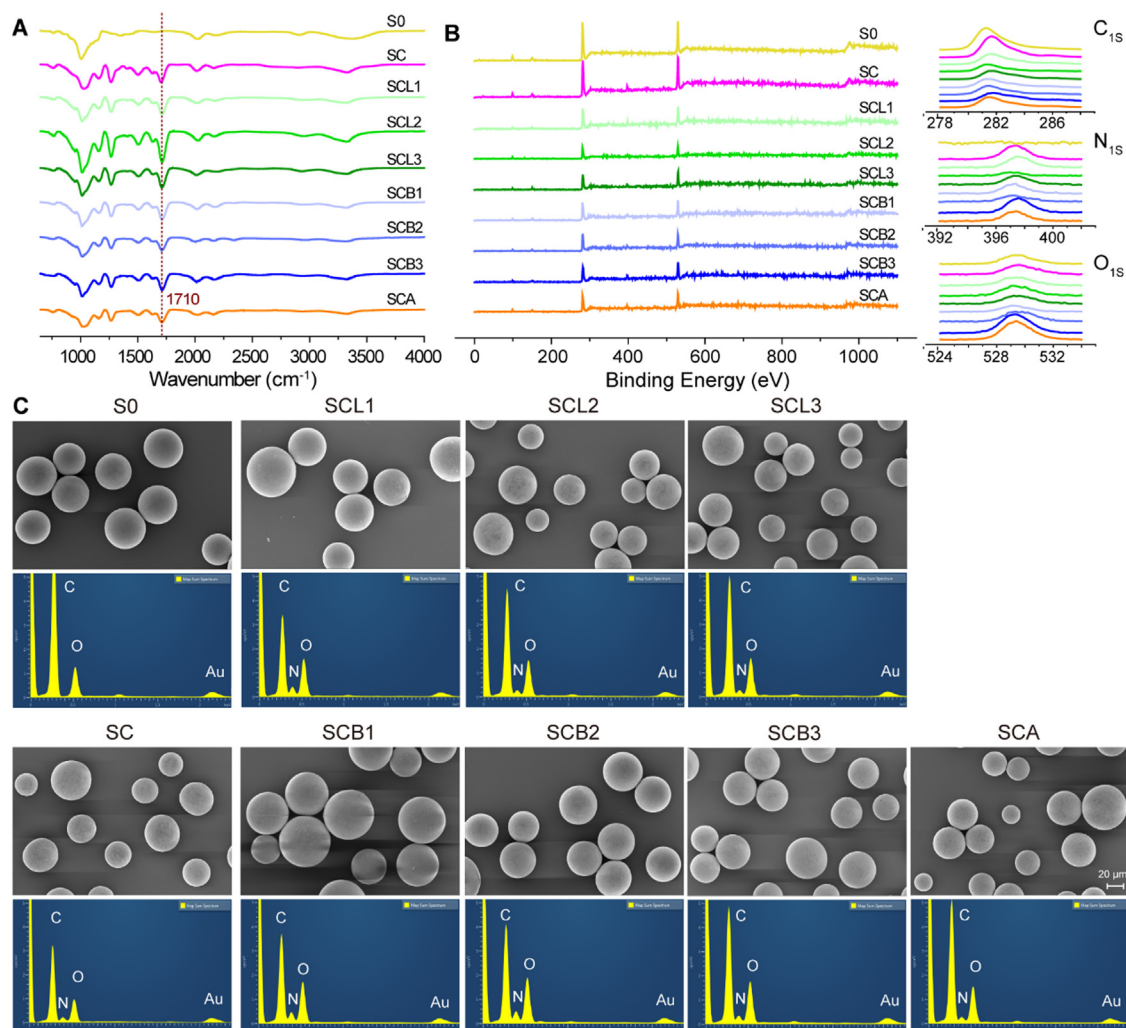


Fig. 2 – Basic characterization of microspheres. (A) FTIR results of microspheres. (B) XPS full spectrum of microspheres and the corresponding C_{1s}, N_{1s}, and O_{1s} spectrum. (C) SEM-EDS results of microspheres.

maintained the same size, even after carbazate modification and hydrophobic modification. It also exhibited the obvious N peaks in SC, SCLs, SCBs and SCA, confirming the successful grafting of carbazate groups as well.

The DS of carbazate was denoted as the content of carbazate groups per dextran unit. The image of S0 and SC after the TNBS assay was shown in Fig. S1. It was obviously observed that the color of SC changed after carbazate modification compared to S0. According to the carbazate standard curve, the carbazate DS of SC was 12.62%. And the DS of SC was 10.87% by XPS, consistent with that of the TNBS assay. The detailed element ratios and the DS of hydrophobic groups were listed in Table S2. It was shown that the DS of hydrophobic S0 was at the range of 5.5%–6.5%.

In addition, the pH stability of SC was investigated by immersing the microspheres in PBS with different pH. As shown in Fig. S2, the absorbance of SC maintained below 0.03 both pH 5.5 and 7.4 buffer, consistent with that of S0. It indicated that carbazate groups maintained relatively stable under physiological (pH 7.4) and weak acid conditions (pH 5.5),

expected to possess favourable stability in both physiological and weak acid OA environments.

3.3. Physical properties of microspheres

Water contact angle (WCA) was applied to characterize the hydrophobic properties of microspheres. As presented in Fig. 3A, WCA was almost 0° for S0, but increased to 36.1° for SC. After aliphatic/aromatic chain modification, the hydrophobicity of microspheres changed sharply. WCA of SCLs increased as following: SCL1 (43.2°) < SCL2 (125.7°) < SCL3 (148.4°) while that of SCBs was in the sequence of SCB1 (55.2°) < SCB2 (133.7°) < SCB3 (165.4°). Significantly, the WCA of SCA dramatically increased to 179.7°, which was the biggest among all the others. For microspheres with different types of hydrophobic modification, it presented the trend of SCL3 < SCB3 < SCA. The superhydrophobicity (WCA > 150°) was achieved by longer branched alkane chain (SCB3) and aromatic group modification (SCA). Besides, the thermal properties of microspheres were explored by TGA. As

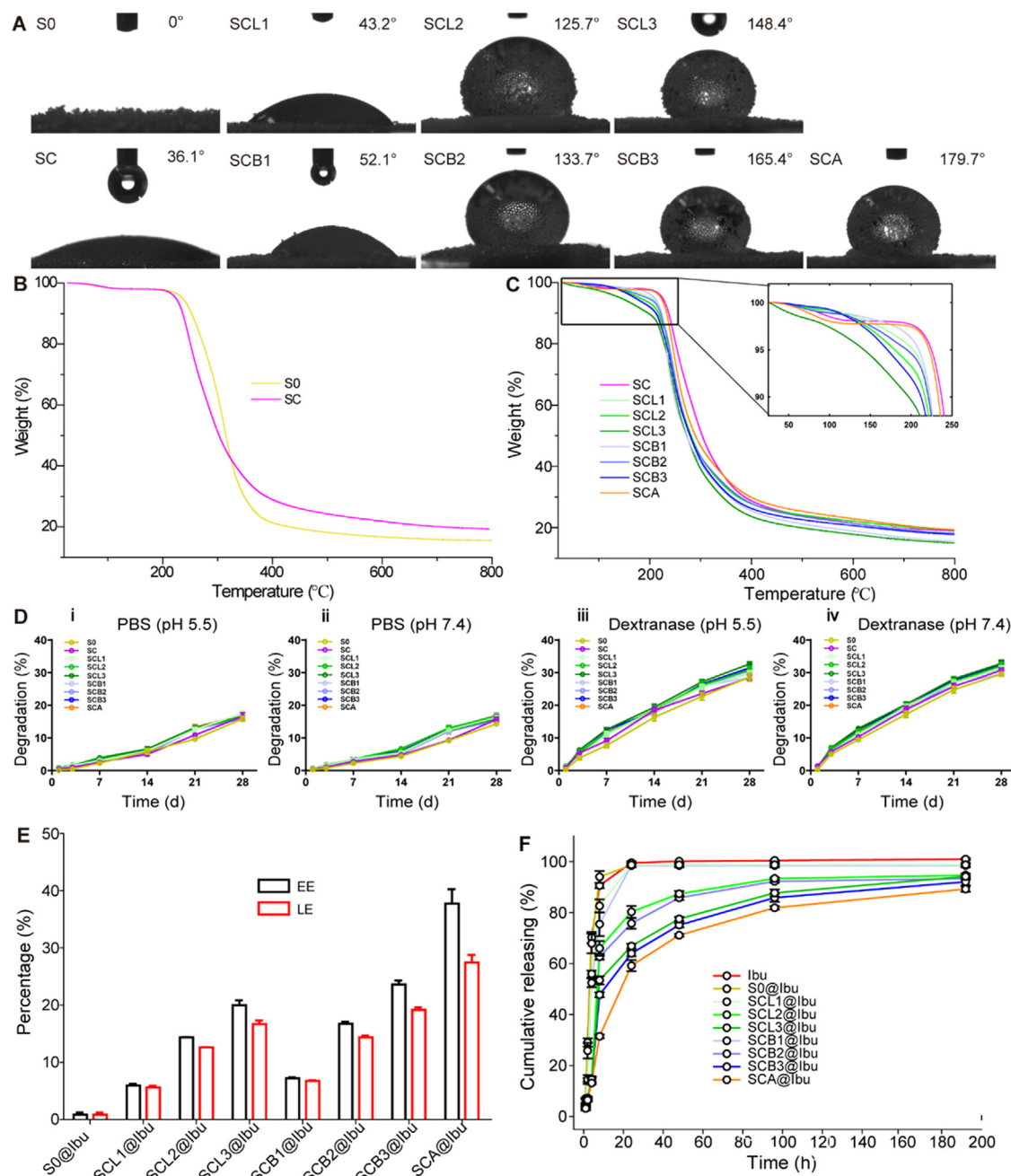


Fig. 3 – Physical properties of microspheres. (A) WCA of microspheres. (B) TGA results of S0 and SC. (C) TGA results of hydrophobic microspheres. (D) The degradation rate of microspheres in vitro: (i) pH 5.5 & (ii) pH 7.4, and (iii) pH 5.5 with dextranase (2 U/ml) & (iv) pH 7.4 with dextranase (2 U/ml). (E) The EE and LE of Ibu on the microspheres. (F) The release rate of Ibu on the microspheres.

presented in Fig. 3B, the decomposition temperature (T_d) of SC was lower than that of S0 after carbazate modification. Kenawy et al. also demonstrated that the introduction of amino groups in chitosan resulted in lower T_d than pristine chitosan [36]. As shown in Fig. 3C, the T_d of hydrophobic microspheres decreased with the increase of linear/branched alkane chains in the order of SCL3 < SCL2 < SCL1 and SCB3 < SCB2 < SCB1, respectively. It also indicated that grafted groups affected the thermal stability of microspheres. As

expected, the thermal stability of microspheres gradually decreased with the increase of the chain length of modified alkanes, which was consistent with the findings of several studies [37]. In general, SCBs exhibited higher T_d than that of SCLs, attributed to stronger molecular interaction between branched alkane groups. Likewise, Demircan et al. confirmed that the introduction of branched polymers increased the thermal stability of cellulose derivatives [38]. Notably, the T_d of SCA increased close to SC. Thus, the T_d of

hydrophobic microspheres showed the trend of SCL3 < SCB3 < SCA.

From the above, it revealed that the introduction of hydrophobic groups distinctly improved the hydrophobic and thermal properties of microspheres. And the length of the alkane chain remarkably affected the hydrophobicity and T_d . The longer alkane chain length corresponded to stronger hydrophobicity and lower T_d , and aromatic hydrocarbon contributed the strongest hydrophobicity and thermal stability followed by branched alkane and linear alkane.

3.4. Degradation rate in vitro

The degradation properties of microspheres were studied by testing their weight changes under different conditions. In Fig. 3D, it exhibited a smooth degradation rate in different PBS (pH 5.5 and 7.4). On Week 4, the degradation rates for microspheres were identical, around 16%. When the microspheres were incubated in PBS (pH 5.5 (iii) and 7.4 (iv)) containing dextranase at 37 °C for 4 weeks, their degradation rates accelerated to about 30%. Although a bit increase in buffer containing dextranase, the degradation rate of hydrophobic microspheres was still extremely lower than most dextran-based hydrogels, which degraded within 18 h [39]. The results demonstrated that the microspheres were gradually degraded under physiological and weak acid conditions (close to an OA environment). To simulate the enzyme environment *in vivo*, the degradation was employed under a dextranase solution. The result showed that it could resist decomposition to some extent, beneficial to maintain sustained drug release.

3.5. Drug loading ratio and release rate

The EE and LE of Ibu-loaded microspheres were investigated respectively. As indicated in Fig. 3E, for S0, the EE and LE were below 1% due to the microporous adsorption of S0. And the EE and LE of Ibu-loaded microspheres increased with the increase of linear/branched alkane chains in the order of SCL1 < SCL2 < SCL3 and SCB1 < SCB2 < SCB3, respectively. In comparison, the EE and LE of Ibu-loaded microspheres were in the order of SCL3 < SCB3 < SCA. Among all microspheres, SCA exhibited the highest EE and LE, with 37.89% and 27.46%, respectively. It revealed that the introduction of hydrophobic groups distinctly improved the EE and LE of microspheres. And the EE and LE increased with the increase of hydrophobicity of microspheres determined by the length of the alkane chain, whatever the linear or branched substitutes. Compared with the alkane chain, the aromatic group remarkably improved the EE and LE of microspheres, mainly attributed to the π - π stacking between Ibu and aromatic groups.

The Ibu release rate was evaluated and illustrated in Fig. 3F. The Ibu suspension in PBS (pH 7.4) was rapidly released from the dialysis tube within 8 h. And the release rate of S0@Ibu was similar to that of Ibu alone. However, for Ibu-loaded microspheres, they exhibited an initial burst effect within 8 h, due to the rapid dissolution of Ibu adsorbed on the micropores of microspheres. The Ibu release rate of

hydrophobic microspheres presented the order of SCL3@Ibu < SCL2@Ibu < SCL1@Ibu and SCB3@Ibu < SCB2@Ibu < SCB1@Ibu, demonstrating the effect of alkane chain length on the drug release rate. For SC with different types of modifications, the Ibu release rate was in the order of SCA@Ibu < SCB3@Ibu < SCL3@Ibu. Among all groups, SCA@Ibu showed excellent sustained drug release. The above results conformed to their hydrophobicity, revealing that the introduction of hydrophobic groups distinctly improved Ibu release behaviors, particularly for the aromatic group. And the Ibu release rate of Ibu-loaded microspheres also strongly depended on the length of the alkane chain. Therefore, the introduction of hydrophobic groups enhanced the interaction between carrier and hydrophobic drugs, beneficial to high drug loading and long-sustained drug release.

3.6. Cell viability assessment

The cytotoxicity of Ibu-loaded microspheres was explored by CCK-8 assay. As shown in i of Fig. 4A, Ibu exhibited little cytotoxicity below the concentration of 200 $\mu\text{g/ml}$. However, the viability of chondrocytes decreased sharply ($P < 0.05$) when the concentration of Ibu increased above 400 $\mu\text{g/ml}$. The Ibu concentration of 200 $\mu\text{g/ml}$ was chosen as the optimal dose for further experiment and the dosage of SCA@Ibu, acted as the maximum Ibu-loaded microspheres, was 728 $\mu\text{g/ml}$ (equivalent concentration of 200 $\mu\text{g/ml}$ Ibu) calculated by the optimal concentration of Ibu. The concentration of other Ibu-loaded microspheres matched that of SCA@Ibu (728 $\mu\text{g/ml}$). All Ibu-loaded microspheres exhibited little cytotoxicity on chondrocytes (ii of Fig. 4A).

The high level of interleukin-1 beta (IL-1 β) contributes to the increased chondrocytes apoptosis, along with the cartilage matrix degradation and further joint inflammation. Thus, it is commonly used to induce inflammation of chondrocytes. The cell viability of IL-1 β induced chondrocytes treated by Ibu-loaded microspheres was also tested by CCK-8 assay (iii of Fig. 4A). It was obviously observed that a decrease of 30.21% for chondrocytes viability was induced by IL-1 β stimulation for 24 h, compared with normal chondrocytes, which demonstrated that IL-1 β exerted mitochondria and DNA damage, leading to chondrocytes apoptosis [26,40,41]. The viability of the S0@Ibu+IL-1 β group was close to the IL-1 β group, indicating that S0 could not act as DDSs. However, SCLs@Ibu increased the cell viability of IL-1 β induced chondrocytes as following: SCL1@Ibu < SCL2@Ibu < SCL3@Ibu. For SCBs@Ibu, the cell viability was in the sequence of SCB1@Ibu < SCB2@Ibu < SCB3@Ibu. Most significantly, Ibu-loaded microspheres improved the cell viability in the order of SCL3@Ibu < SCB3@Ibu < SCA@Ibu. Among all of the groups, SCA@Ibu presented the optimal improvement of cell viability and dramatically increased the cell viability of IL-1 β induced chondrocytes by 29%.

Live/dead assay was also applied to assess the cytotoxicity of chondrocytes. As presented in Fig. 4B and 4C, IL-1 β induced an obvious decrease in live cells (green) and an increase in dead cells (red) with a significantly low live/dead ratio of 7.6. SCLs@Ibu rescued the IL-1 β induced chondrocytes in the order of SCL1@Ibu < SCL2@Ibu < SCL3@Ibu while SCBs@Ibu exhibited similar trends of SCB1@Ibu < SCB2@Ibu <

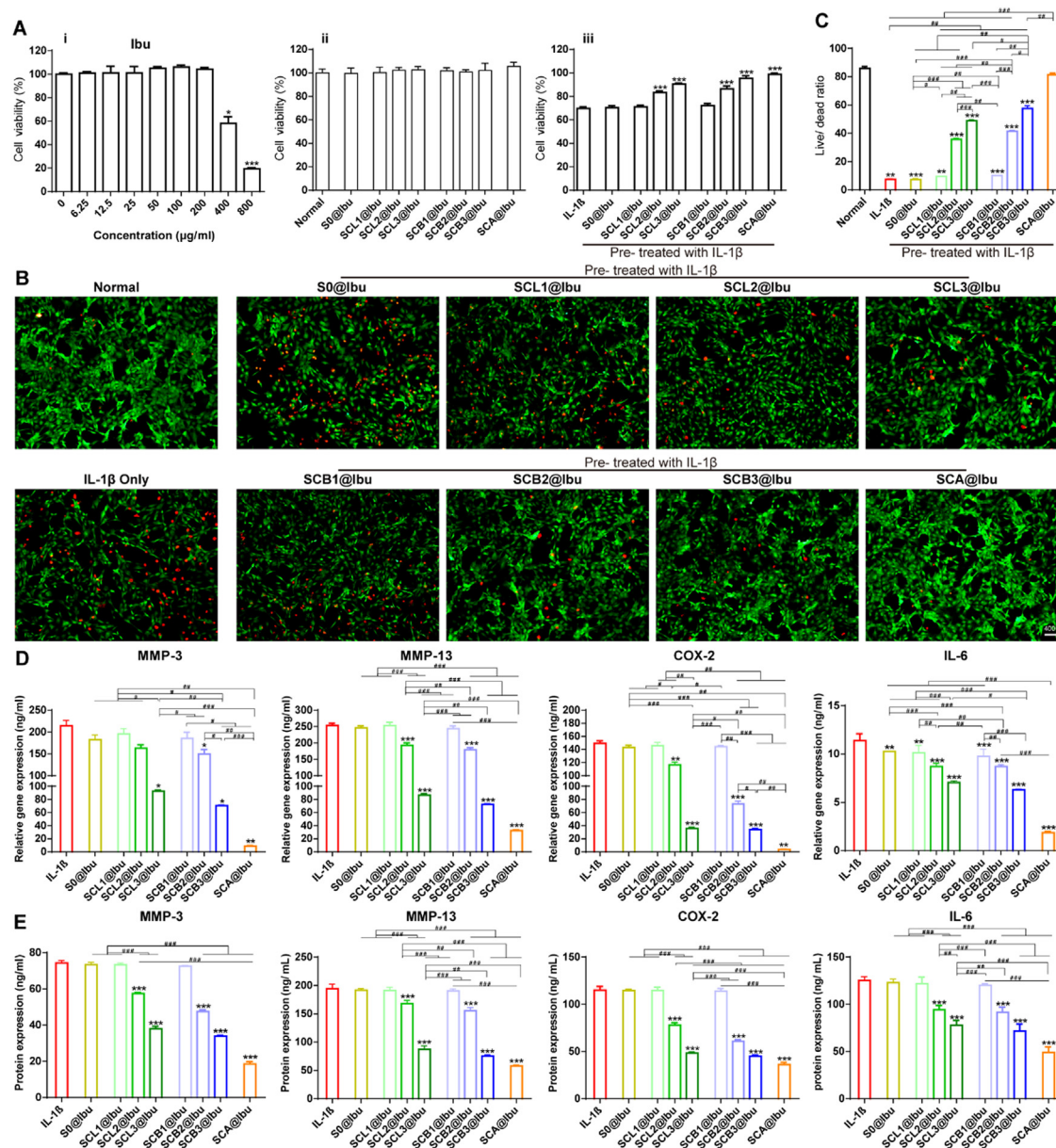


Fig. 4 – The chondrocytes viability and anti-inflammatory effects of Ibu-loaded microspheres. (A) Cytotoxicity of Ibu (i) and Ibu-loaded microspheres (ii) by CCK-8 assay after 24 h. (iii) Cell viability of chondrocytes pre-treated with culture medium only and Ibu-loaded microspheres followed by IL-1 β (10 ng/ml) stimulation for 24 h by CCK-8 assay ($n = 3$, “*” symbol compared with IL-1 β group, ** $P < 0.01$ and * $P < 0.001$); (B) Cell viability of chondrocytes pre-treated with culture medium only, and IL-1 β (10 ng/ml) stimulation for 24 h followed by Ibu-loaded microspheres by Calcein-AM/PI assay. (Scale bar= 400 μ m); (C) Quantification of live/ dead ratio; (D) Gene expression levels of MMP-3, MMP-13, COX-2, and IL-6 in chondrocytes pre-treated with culture medium only, and IL-1 β (10 ng/ml) stimulation for 24 h followed by Ibu-loaded microspheres by qRT-PCR. (E) Protein expression levels of MMP-3, MMP-13, COX-2, and IL-6 in chondrocytes pre-treated with culture medium only, and IL-1 β (10 ng/ml) stimulation for 24 h followed by Ibu-loaded microspheres by ELISA kit. (“*” symbol compared with IL-1 β group, * $P < 0.05$, ** $P < 0.01$ and *** $P < 0.001$, and “#” symbol compared between groups, # $P < 0.05$, ## $P < 0.01$ and ### $P < 0.001$).**

SCB3@Ibu, much higher than that of S0@Ibu. Besides, the live/dead ratio of Ibu-loaded microspheres was in the order of SCL3@Ibu < SCB3@Ibu < SCA@Ibu. Specifically, SCA@Ibu showed the highest live/dead ratio (81.5), demonstrating a positive role in cell growth.

From the above, it revealed that the introduction of hydrophobic groups distinctly improved the Ibu loading efficiency of microspheres, leading to a significant improvement of the viability of IL-1 β induced chondrocytes. Simultaneously, the length of the alkane chain remarkably

affected the Ibu LE of microspheres and thus affected the chondrocytes viability, whatever the linear or branched alkane substitutes. For three different types of modified groups, SCA@Ibu possessed optimal cell viability than that of SCB3@Ibu and SCL3@Ibu. Therefore, hydrophobic modification for microspheres, especially the aromatic group, was beneficial to cell growth by improving the hydrophobicity to maintain long-sustained drug release.

3.7. Chondroprotective effects

The anti-inflammatory effects of Ibu-loaded microspheres were evaluated by qRT-PCR analysis to identify the gene expression levels of inflammatory markers (MMP-3, MMP-13, COX-2, and IL-6). As shown in Fig. 4D, IL-1 β stimulation dramatically upregulated the expression levels of MMP-3, MMP-13, COX-2 and IL-6. And S0@Ibu hardly decreased the expression of inflammation regulators. However, SCLs@Ibu decreased the expression of the above inflammatory markers in the order of SCL1@Ibu < SCL2@Ibu < SCL3@Ibu. And SCBs@Ibu also showed similar effects in the sequence of SCB1@Ibu < SCB2@Ibu < SCB3@Ibu. Most importantly, Ibu-loaded microspheres decreased the inflammatory gene expression in the order of SCL3@Ibu < SCB3@Ibu < SCA@Ibu. Specifically, SCA@Ibu dramatically down-regulated the gene expression of MMP-3, MMP-13, COX-2 and IL-6, by 95.81%, 87.23%, 97.39% and 83.43%, respectively.

In the meantime, the protein expression levels of inflammation factors (MMP-3, MMP-13, COX-2, and IL-6) in chondrocytes stimulated with IL-1 β were further evaluated by ELISA kit. As presented in Fig. 4E, it dramatically elevated the expression levels of MMP-3, MMP-13, COX-2, and IL-6 by IL-1 β stimulation. And S0@Ibu had little effect on the inflammation factors. However, SCLs@Ibu attenuated the expression of the above inflammation proteins as following: SCL1@Ibu < SCL2@Ibu < SCL3@Ibu while SCBs@Ibu exhibited similar trends in the order of SCB1@Ibu < SCB2@Ibu < SCB3@Ibu. In comparison, Ibu-loaded microspheres decreased the inflammation proteins expression in the order of SCL3@Ibu < SCB3@Ibu < SCA@Ibu. After statistical calculation, SCA@Ibu significantly attenuated the protein expression of MMP-3, MMP-13, COX-2 and IL-6 by 75.12%, 70.33%, 68.51% and 60.92%, respectively.

The morphology changes of chondrocytes induced with IL-1 β were observed by HE staining. From Fig. 5A, normal chondrocytes with round or polygonal shapes changed to elongated and spindle-like shapes after treatment with IL-1 β for 24 h, indicating the successful induction of OA chondrocytes. S0@Ibu had little effect on the morphology of OA chondrocytes. Conversely, more round or polygonal cells, a typical characteristic of chondrocytes, were observed for SCLs@Ibu, SCBs@Ibu, and SCA@Ibu, suggesting the protective effects on IL-1 β injured chondrocytes. Especially, among all groups, the most round or polygonal cells were observed for SCA@Ibu.

The effects of Ibu-loaded microspheres on GAG secretion of chondrocytes were also investigated by Safranin-O staining (Fig. 5B). The IL-1 β induction led to the negative staining (faint red) in chondrocytes, similar to that of the S0@Ibu. However, SCLs/ SCBs@Ibu showed intense positive staining

(red) in the order of SCL1@Ibu < SCL2@Ibu < SCL3@Ibu and SCB1@Ibu < SCB2@Ibu < SCB3@Ibu. And the highest secretion of GAG was SCA@Ibu. In addition, the ratio of GAG/DNA content was further assessed for the GAG secretion of IL-1 β induced chondrocytes. As presented in Fig. 5C, the DNA content was consistent with the results of cell viability, demonstrating the potent protective roles of cells by hydrophobic microspheres. In Fig. 5D, the ratio of GAG/DNA content in chondrocytes dramatically decreased after IL-1 β stimulation or S0@Ibu. However, the hydrophobic microspheres showed the increasing trend of SCL1@Ibu < SCL2@Ibu < SCL3@Ibu, SCB1@Ibu < SCB2@Ibu < SCB3@Ibu, and SCL3@Ibu < SCB3@Ibu < SCA@Ibu, in agreement with the Safranin-O staining results.

Immunofluorescent staining was also performed to identify the protein expression of inflammatory markers (MMP-13 and IL-6) in IL-1 β induced chondrocytes. As illustrated in Fig. 5E-5H, the intense green fluorescence of MMP-13 or IL-6 was shown in the IL-1 β group. S0@Ibu hardly weakened the fluorescence. But SCLs/ SCBs@Ibu weakened the degree of fluorescence in a sequence of SCL1@Ibu < SCL2@Ibu < SCL3@Ibu and SCB1@Ibu < SCB2@Ibu < SCB3@Ibu. Comparatively, Ibu-loaded microspheres weakened the fluorescence in the order of SCL3@Ibu < SCB3@Ibu < SCA@Ibu. Among all groups, SCA@Ibu extremely weakened the fluorescence most prominent, with only 5.63% and 4.67% positive staining for MMP-13 and IL-6, respectively.

To sum up, the above results demonstrated that the introduction of hydrophobic groups for Ibu-loaded microspheres distinctly improved the anti-inflammatory and chondroprotective effects after IL-1 β stimulation. The length of the alkane chain remarkably affected the LE of microspheres and thus affected anti-inflammatory and chondroprotective effects, whatever the linear or branched alkane substitutes. For the three types of modified groups, SCA@Ibu possessed the optimal anti-inflammatory effects and chondroprotective effects than those of SCB3@Ibu and SCL3@Ibu, conforming to the results of LE and release rate. Therefore, modified with hydrophobic groups, especially the aromatic group, the microspheres were beneficial to anti-inflammation and chondroprotection *in vitro*.

3.8. OA therapy in vivo

To observe the effects of Ibu-loaded microspheres in the articular cavity, we carried out preliminary pharmacokinetic experiments. As shown in Fig. 6B, the concentration-time curves of the Ibu group were markedly different from those of the Ibu-loaded microspheres groups. The concentration of group Ibu was rather high in the initial stage but subsequently decreased dramatically and could not be measured at 24 h after injection. However, the concentration of Ibu-loaded microspheres groups gradually decreased and maintained to 96 h, except for S0@Ibu. Among Ibu-loaded microspheres groups, the release rate trends of three microspheres modified groups were roughly similar, and the ranks (from high to low) of concentration and the area under the curve (AUC) were SCA@Ibu, SCB3@Ibu, SCL3@Ibu, S0@Ibu, in accordance with their drug loading capacities. Noticeably, the S0@Ibu had the lowest concentration in the initial stage and could

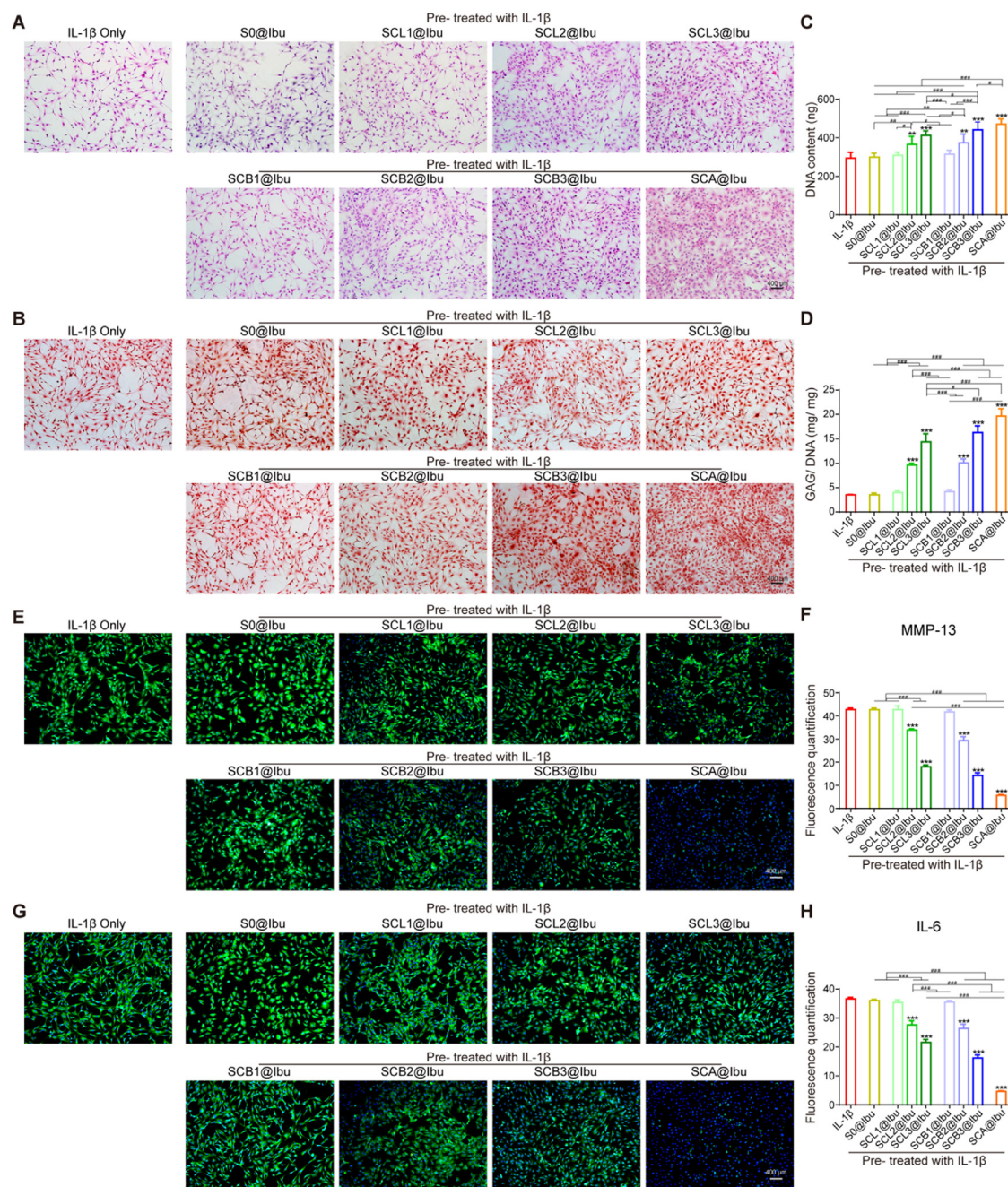


Fig. 5 – Protective effects of Ibu-loaded microspheres on IL-1 β induced chondrocytes. (A) HE staining. (B) Safranin-O staining. (C) The corresponding DNA content (ng). (D) GAG content (mg) normalized to DNA (mg). (E) Immunofluorescent staining of MMP-13 (FITC channel) and the corresponding quantified results (F). (G) Immunofluorescent staining of IL-6 (FITC channel) and the corresponding quantified results (H). (“*” symbol compared with IL-1 β group, * $P < 0.05$, ** $P < 0.01$ and * $P < 0.001$, and “#” symbol compared between groups, # $P < 0.05$, ## $P < 0.01$ and ### $P < 0.001$).**

not be measured at 24 h after injection, due to its poor drug loading capacities. The result indicated that hydrophobic modification improves drug loading capacities and sustained release effects, further reducing the frequency of injection and enhancing the bioavailability.

After the IA injection, rats were sacrificed and the knee joints were harvested on Week 2 and 4. The expression levels of inflammatory markers (MMP-13 and IL-6) in the joint

fluid were measured using the ELISA kit. As illustrated in Fig. 6A, the expression levels of MMP-13 and IL-6 significantly increased in a time-dependent manner for the saline group, which proved the successful establishment of OA model after ACLT surgery. S0@Ibu hardly decreased the levels of both two inflammatory markers on Week 2 and 4. However, Ibu-loaded microspheres decreased the above inflammatory markers in the order of SCL3@Ibu < SCB3@Ibu < SCA@Ibu. Significantly,

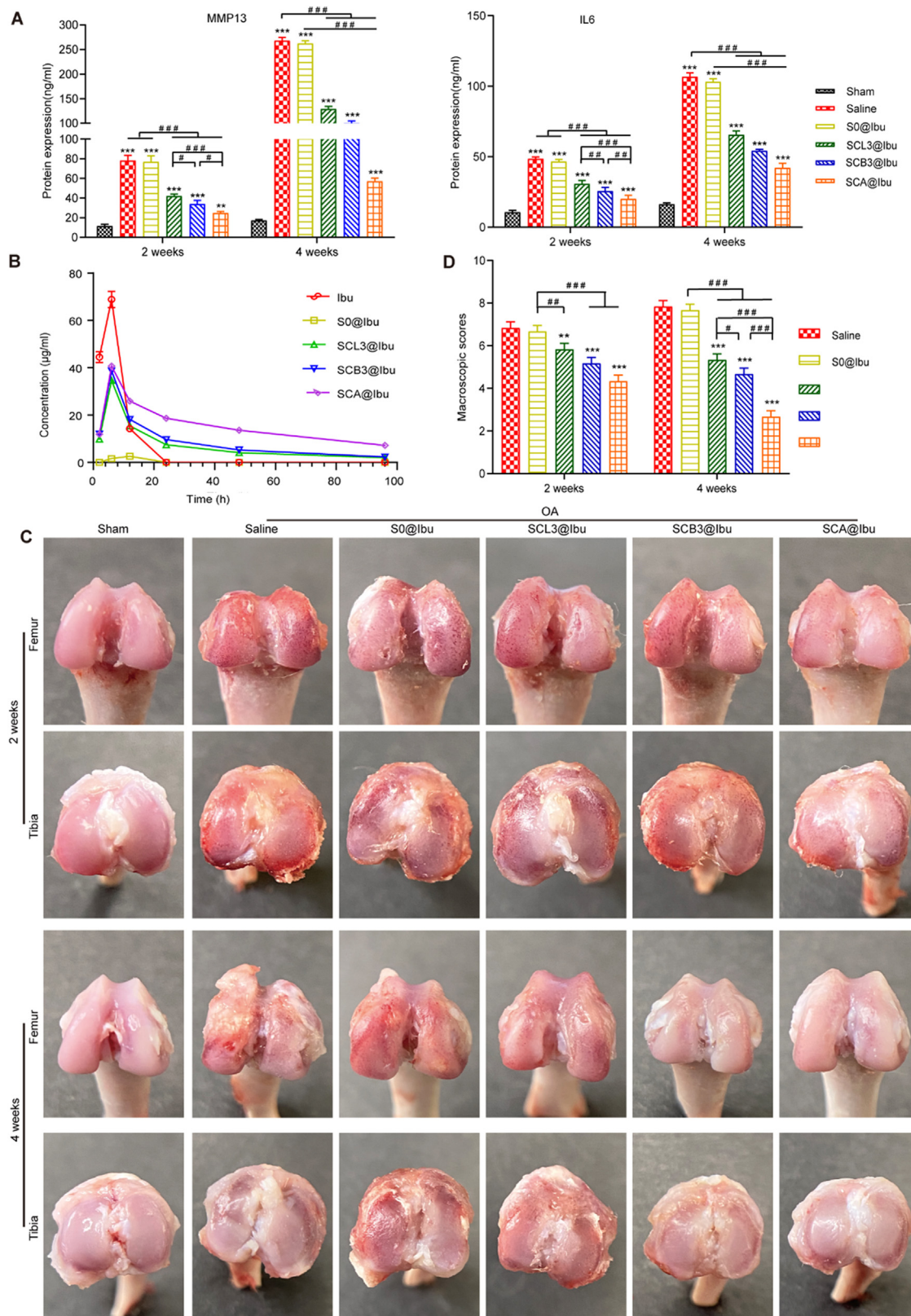


Fig. 6 – The effect of Ibu-loaded microspheres on OA progression in vivo. (A) The protein expression levels of inflammatory factors (MMP-13 and IL-6) in synovial fluid. (B) The retention time of the drug in vivo. (C) Macroscopic observations and the corresponding macroscopic score (D). (“**” symbol compared with saline group, * $P < 0.05$, ** $P < 0.01$ and *** $P < 0.001$, and “#” symbol compared between groups, # $P < 0.05$, ## $P < 0.01$ and ### $P < 0.001$).

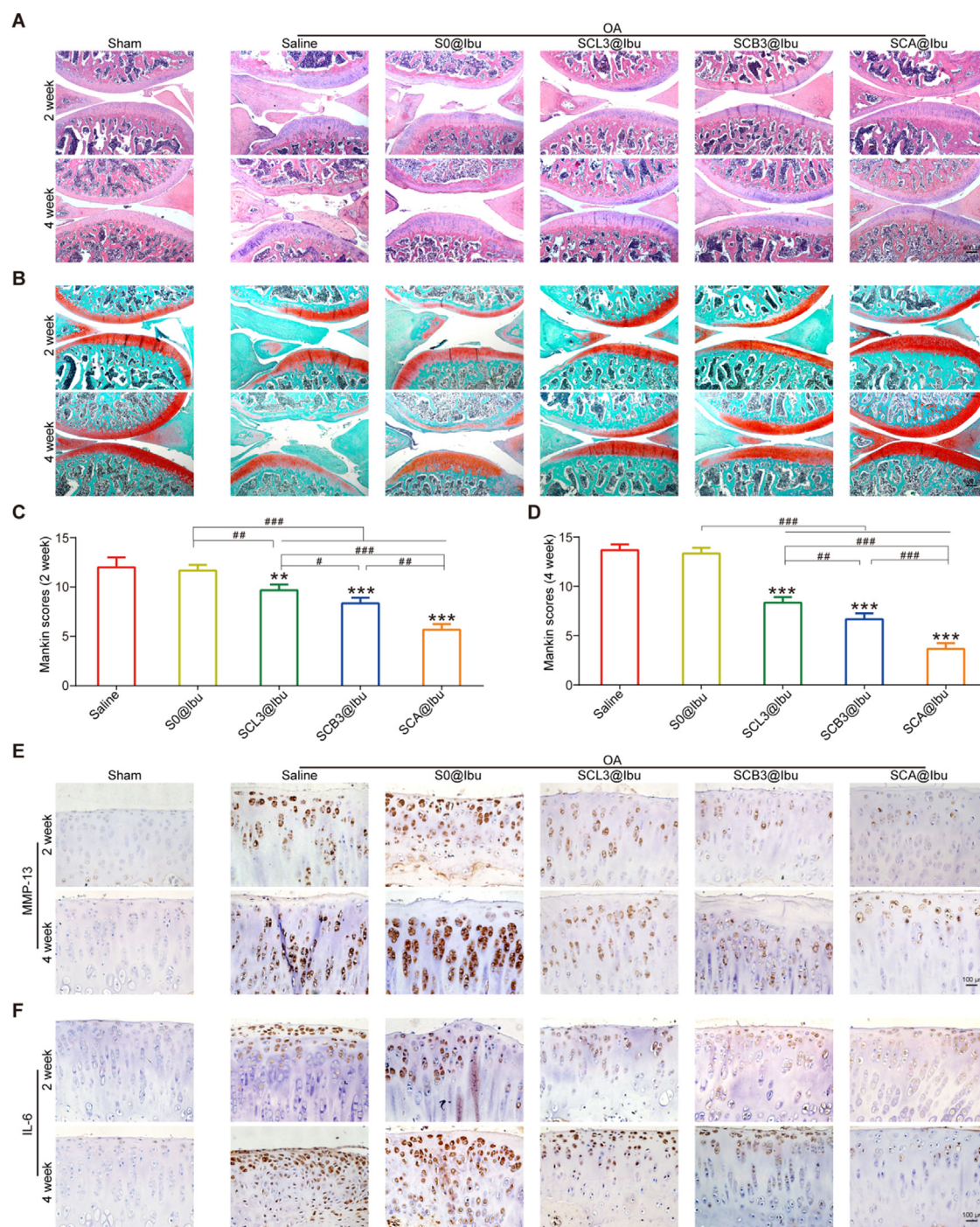


Fig. 7 – Histological analysis of OA treatment effects by Ibu-loaded microspheres. HE staining(A). Safranin-O fast green staining (B) and the corresponding histological scoring at week 2 (C) and week 4 (D). (“*” symbol compared with saline group, *P < 0.05, **P < 0.01 and *P < 0.001, and “#” symbol compared between groups, #P < 0.05, ##P < 0.01 and ###P < 0.001). (E) Immunohistochemical staining of MMP-13. (F) Immunohistochemical staining of IL-6.**

SCA@Ibu decreased the levels of MMP-13 the most, which showed a decrease of 68.26% on Week 2 and 78.76% on Week 4. And SCA@Ibu also decreased the level of IL-6 by ~60% both on Week 2 and 4, the most dramatic for all of the groups.

In Fig. 6C, macroscopic results in knee joints showed that the intact, smooth and glittering surface of articular cartilage was observed for the sham group (normal group). The erosion

denudation of cartilage and formation of osteophyte around peripheral joints were observed for the saline group (OA group), which deteriorated *versus* time. And the macroscopic observation for S0@Ibu was similar to that of the saline group, suggesting that S0@Ibu had hardly a therapeutic effect on OA. Compared with the saline group, SCA@Ibu significantly improved the degeneration of articular cartilage

with a score decline of 36.59% and 65.96% on Week 2 and 4, respectively (Fig. 6D). SCL3@Ibu and SCB3@Ibu also suppressed the progression of OA, but their therapeutic effects were not so prominent as that of SCA@Ibu.

Besides, the histological investigation by HE and Safranin-O fast green staining was conducted to evaluate the changes of articular cartilage (Fig. 7A and 7B). The histological characteristics including fissures, fibrillation, increase of heteromorphic cells, and extensive loss of GAG, were identified in saline and S0@Ibu, which became worsen *versus* time. However, the restoration of cartilage damage and proteoglycan retention was observed after treatment with SCL3@Ibu, SCB3@Ibu and SCA@Ibu, respectively. Among them, SCA@Ibu showed the optimal therapeutic effects with the restoration of cartilage structure, and the most remarkable and consistent Safranin-O staining. In comparison, the three groups were scored in the order of SCL3@Ibu < SCB3@Ibu < SCA@Ibu (Fig. 7C and 7D). Among all groups, SCA@Ibu led to about 52.78% and 73.17% reduction of the score on Week 2 and 4, respectively.

Furthermore, the expression levels of MMP-13 and IL-6 in cartilage tissue on week 2 and week 4 were also measured by immunohistochemical staining (Fig. 7E and 7F). Intense positive staining (brown granules) of MMP-13 and IL-6 was observed for saline and S0@Ibu. By contrast, less positive staining was illustrated for SCL3@Ibu and SCB3@Ibu. Particularly, only negative staining of MMP-13 and IL-6 was exhibited in SCA@Ibu, close to the sham group. It also indicated that SCA@Ibu inhibited the expression of inflammatory cytokines, the most remarkable biomarker in injured articular cartilage.

In general, the above results revealed that the OA therapeutic effect of SCA@Ibu was the most prominent among all of the groups, followed by SCB3@Ibu and SCL3@Ibu. The anti-inflammatory and cartilage protective effects *in vivo* agreed with the results of LE, release behaviors and *in vitro* studies. Thus, the hydrophobic group, especially aromatic hydrocarbon modification for microspheres showed potent anti-inflammatory and chondroprotective effects on OA by high drug loading ratio.

Furthermore, we explored whether Ibu-loaded microspheres had an impact on the major organs of rats by histopathological evaluation after treatment for 4 weeks (Fig. S3). No obvious damage was observed from HE staining of the heart, liver, spleen, lung and kidney. It revealed that microspheres presented a highly safe and effective platform for OA therapy.

4. Conclusions

In this study, a series of hydrophobic modified Sephadex microspheres were innovatively fabricated by carbazate-mediated Schiff-base reaction as DDSs for OA therapy. The results demonstrated that the introduction of hydrophobic groups distinctly improved the hydrophobicity of microspheres and further increased the Ibu loading efficiency, leading to significant improvement of anti-inflammatory and chondroprotective effects *in vitro* and *in vivo*. And the length of the alkane chain remarkably affected

the Ibu loading efficiency and thus affected the biological functions, whatever linear or branched alkane substitutes. Significantly, the aromatic group modified microsphere presented the superhydrophobicity, highest drug loading ratio, and optimal anti-inflammatory and chondroprotective effects. Besides, the hydrophobic microspheres degraded slowly and maintained a long retention time in the joint cavity. In summary, modification by hydrophobic groups, especially aromatic hydrocarbon for microspheres improved the behavior of sustained drug release, finally leading to improved OA therapeutic effects.

Conflicts of interest

The authors declare that no potential conflicts of interest were disclosed.

Acknowledgments

The work was financially supported by National Natural Science Foundation of China (Grant No. 82160430), Natural Science Foundation of Guangxi (Grant No. 2020GXNSFAA159134 and 2019GXNSFAA185060), Guangxi Science and Technology Base and Talent Special Project (Grant No. GuikeAD19254003 and GuikeAD21075002), and Nanning Qingxiu District Science and Technology Major Special Project (Grant No. 2020013).

Supplementary materials

Supplementary material associated with this article can be found, in the online version, at [doi:10.1016/j.ajps.2023.100830](https://doi.org/10.1016/j.ajps.2023.100830).

REFERENCES

- [1] Hunter DJ, Bierma-Zeinstra S. Osteoarthritis. *Lancet North Am Ed* 2019;393(10182):1745–59.
- [2] Zheng L, Zhang Z, Sheng P, Mobasher A. The role of metabolism in chondrocyte dysfunction and the progression of osteoarthritis. *Ageing Res Rev* 2021;66:101249.
- [3] Tian J, Yao C, Yang WL, Zhang L, Zhang DW, Wang H, et al. *In situ*-prepared homogeneous supramolecular organic framework drug delivery systems(soft-DDSs):overcoming cancer multidrug resistance and controlled release. *Chin Chem Lett* 2017;28(04):798–806.
- [4] Nguyen C, Rannou F. The safety of intra-articular injections for the treatment of knee osteoarthritis: a critical narrative review. *Expert Opin Drug Saf* 2017;16(8):897–902.
- [5] Jones IA, Togashi R, Wilson ML, Heckmann N, Vangsness CT. Intra-articular treatment options for knee osteoarthritis. *Nat Rev Rheumatol* 2019;15(2):77–90.
- [6] DeJulius CR, Gulati S, Hasty KA, Crofford LJ, Duvall CL. Recent advances in clinical translation of intra-articular osteoarthritis drug delivery systems. *Adv Ther* 2021;4(1):2000088.
- [7] Mwangi TK, Berke IM, Nieves EH, Bell RD, Adams SB, Setton LA. Intra-articular clearance of labeled dextrans from naive and arthritic rat knee joints. *J Controlled Release* 2018;283:76–83.

- [8] Evans CH, Kraus VB, Setton LA. Progress in intra-articular therapy. *Nat Rev Rheumatol* 2014;10(1):11–22.
- [9] Maudens P, Jordan O, Allémann E. Recent advances in intra-articular drug delivery systems for osteoarthritis therapy. *Drug Discov Today* 2018;23(10):1761–75.
- [10] Bowman S, Awad ME, Hamrick MW, Hunter M, Fulzele S. Recent advances in hyaluronic acid based therapy for osteoarthritis. *Clin Transl Med* 2018;7(1):6.
- [11] Chen P, Xia C, Mei S, Wang J, Shan Z, Lin X, et al. Intra-articular delivery of sinomenium encapsulated by chitosan microspheres and photo-crosslinked GelMA hydrogel ameliorates osteoarthritis by effectively regulating autophagy. *Biomaterials* 2016;81:1–13.
- [12] She P, Bian X, Cheng Y, Dong S, Liu J, Liu W, et al. Dextran sulfate-triamcinolone acetonide conjugate nanoparticles for targeted treatment of osteoarthritis. *Int J Biol Macromol* 2020;158:1082–9.
- [13] Han Y, Yang J, Zhao W, Wang H, Sun Y, Chen Y, et al. Biomimetic injectable hydrogel microspheres with enhanced lubrication and controllable drug release for the treatment of osteoarthritis. *Bioact Mater* 2021;6(10):3596–607.
- [14] Tezel A, Fredrickson GH. The science of hyaluronic acid dermal fillers. *J Cosmet Laser Ther* 2008;10(1):35–42.
- [15] Sulistio A, Mansfeld FM. Intra-articular treatment of osteoarthritis with diclofenac-conjugated polymer reduces inflammation and pain. *ACS Appl Bio Mater* 2019;2(7):2822–32.
- [16] Seong YJ, Lin G, Kim BJ, Kim HE, Kim S, Jeong SH. Hyaluronic acid-based hybrid hydrogel microspheres with enhanced structural stability and high injectability. *ACS Omega* 2019;4(9):13834–44.
- [17] Hou X, Liu Y. Preparation and drug controlled release of porous octyl-dextran microspheres. *J Biomater Sci Polym Ed* 2015;26(15):1051–66.
- [18] Yang DY, Ko K, Lee SH, Moon DG, Kim JW, Lee WK. Efficacy and safety of newly developed cross-linked dextran gel injection for glans penis augmentation with a novel technique. *Asian J Androl* 2018;20(1):80–4.
- [19] Moghadam Ariaee F, Tafaghodi M. Mucosal adjuvant potential of quillaja saponins and cross-linked dextran microspheres, co-administered with liposomes encapsulated with tetanus toxoid. *IJPR* 2012;11(3):723–32.
- [20] Mahajan HS, Gundare SA. Preparation, characterization and pulmonary pharmacokinetics of xyloglucan microspheres as dry powder inhalation. *Carbohydr Polym* 2014;102:529–36.
- [21] Vlugt-Wensink KD, Jiang X, Schotman G, Kruijtzter G, Vredenberg A, Chung JT, et al. *In vitro* degradation behavior of microspheres based on cross-linked dextran. *Biomacromolecules* 2006;7(11):2983–90.
- [22] Liu J, Qi C, Tao K, Zhang J, Zhang J, Xu L, et al. Sericin/dextran injectable hydrogel as an optically trackable drug delivery system for malignant melanoma treatment. *ACS Appl Mater Interfaces* 2016;8(10):6411–22.
- [23] Pirouzmand H, Khameneh B, Tafaghodi M. Immunoadjuvant potential of cross-linked dextran microspheres mixed with chitosan nanospheres encapsulated with tetanus toxoid. *Pharm Biol* 2017;55(1):212–17.
- [24] Payne WM, Svehckarev D, Kyrychenko A, Mohs AM. The role of hydrophobic modification on hyaluronic acid dynamics and self-assembly. *Carbohydr Polym* 2018;182:132–41.
- [25] Mohan T, Rathner R, Reishofer D, Koller M, Elschner T, Spirk S, et al. Designing hydrophobically modified polysaccharide derivatives for highly efficient enzyme immobilization. *Biomacromolecules* 2015;16(8):2403–11.
- [26] Alexander S, Eastoe J, Lord AM, Guittard F, Barron AR. Branched hydrocarbon low surface energy materials for superhydrophobic nanoparticle derived surfaces. *ACS Appl Mater Interfaces* 2016;8(1):660–6.
- [27] Chen X, Taguchi T. Enhanced skin adhesive property of hydrophobically modified poly(vinyl alcohol) films. *ACS Omega* 2020;5(3):1519–27.
- [28] Alexander S, Smith GN, James C, Rogers SE, Guittard F, Sagisaka M, et al. Low-surface energy surfactants with branched hydrocarbon architectures. *Langmuir* 2014;30(12):3413–21.
- [29] Cho E, Tahir MN, Choi JM, Kim H, Yu JH, Jung S. Novel magnetic nanoparticles coated by benzene- and β -cyclodextrin-bearing dextran, and the sorption of polycyclic aromatic hydrocarbon. *Carbohydr Polym* 2015;133:221–8.
- [30] Sedaghat Doost A, Nikbakht Nasrabadi M, Goli SAH, van Troys M, Dubruel P, De Neve N, et al. Maillard conjugation of whey protein isolate with water-soluble fraction of almond gum or flaxseed mucilage by dry heat treatment. *Food Res Int* 2020;128:108779.
- [31] Yang Y, Gao M, Zhou B, Cai P, Larsson TE, Zhao J, et al. Weak acidic stable carbazate modified cellulose membranes target for scavenging carbonylated proteins in hemodialysis. *Carbohydr Polym* 2020;231:115727.
- [32] Zhong G, Yang X, Jiang X, Kumar A, Long H, Xie J, et al. Dopamine-melanin nanoparticles scavenge reactive oxygen and nitrogen species and activate autophagy for osteoarthritis therapy. *Nanoscale* 2019;11(24):11605–16.
- [33] Jiang T, Kai D, Liu S, Huang X, Heng S, Zhao J, et al. Mechanically cartilage-mimicking poly (PCL-PTHF urethane)/collagen nanofibers induce chondrogenesis by blocking NF-kappa B signaling pathway. *Biomaterials* 2018;178:281–92.
- [34] Pelletier JP, Fernandes JC, Brunet J, Moldovan F, Schrier D, Flory C, et al. *In vivo* selective inhibition of mitogen-activated protein kinase kinase 1/2 in rabbit experimental osteoarthritis is associated with a reduction in the development of structural changes. *Arthritis Rheum* 2003;48(6):1582–93.
- [35] Pritzker KP, Gay S, Jimenez SA, Ostergaard K, Pelletier JP, Revell PA, et al. Osteoarthritis cartilage histopathology: grading and staging. *Osteoarthr Cartil* 2006;14(1):13–29.
- [36] Kenawy ER, Ali SS, Al-Etewy M, Sun J, Wu J, El-Zawawy N. Synthesis, characterization and biomedical applications of a novel Schiff base on methyl acrylate-functionalized chitosan bearing p-nitrobenzaldehyde groups. *Int J Biol Macromol* 2019;122:833–43.
- [37] Sealey JE, Samaranayake G, Todd JG, Glasser WG. Novel cellulose derivatives. IV. Preparation and thermal analysis of waxy esters of cellulose. *J Polym Sci Part B* 1996;34:93.
- [38] Demircan D, Zhang B. Facile synthesis of novel soluble cellulose-grafted hyperbranched polymers as potential natural antimicrobial materials. *Carbohydr Polym* 2017;157:1913–21.
- [39] Chiu HC, Hsiue GH, Lee YP, Huang LW. Synthesis and characterization of pH-sensitive dextran hydrogels as a potential colon-specific drug delivery system. *J Biomater Sci, Polym Ed* 1999;10(5):591–608.
- [40] Yasuhara R, Miyamoto Y, Akaike T, Akuta T, Nakamura M, Takami M, et al. Interleukin-1beta induces death in chondrocyte-like ATDC5 cells through mitochondrial dysfunction and energy depletion in a reactive nitrogen and oxygen species-dependent manner. *Biochem J* 2005;389(Pt 2):315–23.
- [41] Cai C, Min S, Yan B, Liu W, Yang X, Li L, et al. MiR-27a promotes the autophagy and apoptosis of IL-1 β treated-articular chondrocytes in osteoarthritis through PI3K/AKT/mTOR signaling. *Aging* 2019;11(16):6371–84.